Poly-dopamine, poly-levodopa, and poly-norepinephrine coatings: Comparison of physico-chemical and biological properties with focus on the application for blood-contacting devices

Xing Tan[a,1], Peng Gao[a,1], Yalong Li[b], Pengkai Qi[a], Jingxia Liu[c], Ru Shen[a], Lianghui Wang[a], Nan Huang[a], Kaiqin Xiong[a,***], Wenjie Tian[d,**], Qiufen Tu[a,*]

[a] Key Lab of Advanced Technology of Materials of Education Ministry, Southwest Jiaotong University, Chengdu, 610031, China
[b] Department of Stem Cell Center, Henan Key Laboratory of Stem Cell Differentiation and Modification, Henan Provincial People's Hospital; People's Hospital of Zhengzhou University, Zhengzhou, Henan, 450003, China
[c] Physical Education Department, Southwest Jiaotong University, Chengdu, 610031, China
[d] Cardiology Department, Sichuan Academy of Medical Sciences & Sichuan Provincial People's Hospital, School of Medicine, University of Electronic Science and Technology of China. 32 West Second Section, First Ring Road, Chengdu 610072, China

ABSTRACT

Thanks to its simplicity, versatility, and secondary reactivity, dopamine self-polymerized coatings (pDA) have been widely used in surface modification of biomaterials, but the limitation in secondary molecular grafting and the high roughness restrain their application in some special scenarios. Therefore, some other catecholamine coatings analog to pDA have attracted more and more attention, including the smoother poly-norepinephrine coating (pNE), and the poly-levodopa coating (pLD) containing additional carboxyl groups. However, the lack of a systematic comparison of the properties, especially the biological properties of the above three catecholamine coatings, makes it difficult to give a guiding opinion on the application scenarios of different coatings. Herein, we systematically studied the physical, chemical, and biological properties of the three catecholamine coatings, and explored the feasibility of their application for the modification of biomaterials, especially cardiovascular materials. Among them, the pDA coating was the roughest, with the largest amount of amino and phenolic hydroxyl groups for molecule grafting, and induced the strongest platelet adhesion and activation. The pLD coating was the thinnest and most hydrophilic but triggered the strongest inflammatory response. The pNE coating was the smoothest, with the best hemocompatibility and histocompatibility, and with the strongest cell selectivity of promoting the proliferation of endothelial cells while inhibiting the proliferation of smooth muscle cells. To sum up, the pNE coating may be a better choice for the surface modification of cardiovascular materials, especially those for vascular stents and grafts, but it is still not widely recognized.

1. Introduction

Polydopamine (pDA) coatings, inspired by the adhesion behavior of mussels, were firstly introduced by Lee et al., in 2007, and since then opened up a new field of material surface modification [1], thanks to their simplicity, versatility, and secondary reactivity. Firstly, the coating can be simply formed by oxidation and self-polymerization of dopamine (DA) in aerated alkaline solution. Secondly, the coating can be versatilely deposited onto a variety of materials, whether hydrophilic [2] or hydrophobic [3]; whether blocky [4], filamentous [5] or granular [6]; whether metal [7], polymer [8] or even a living cell [9]. And finally, via Michael addition or Schiff base reaction based on phenolic hydroxyl or quinone groups, the PDA coating can be conjugated with some active molecules containing sulfhydryl (-SH) or amino (-NH$_2$) groups [10]. Despite the extensive use of pDA coating, some uncontrollable factors in the process of self-polymerization may
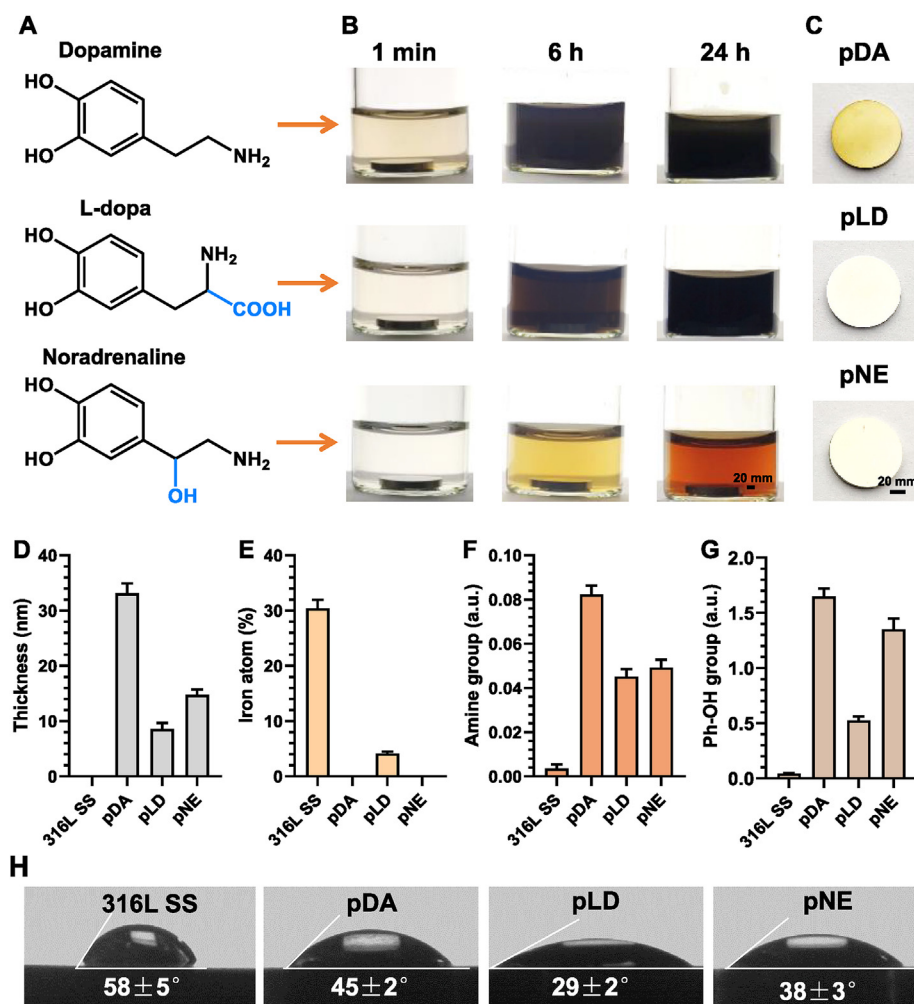
Fig. 1. Preparation and physicochemical characterization of catecholamine coatings on 316 L SS substrates. (A) Molecule structures of DA, LD, and NE. (B) The image of the reactive solution after disposition for 1 min, 6 h, and 24 h, respectively. (C) 24 h coated 316 L SS substrates, after washing and drying. (D) The thickness of the catecholamine coating on 316 L SS substrates determined by spectroscopic ellipsometry. (E) Iron atom percentage of these coating on the 316 L SS substrates. (F) The density of amine groups on the catecholamine coatings. (G) The density of phenolic hydroxyl groups on these coatings surface. (H) Static water contact angles of the catecholamine coating surface.

limit its application in some fields. For example, the significant increase in surface roughness of pDA coatings caused by the inevitable aggregation of oligo-DA micro-/nano-particles may limit their application in some fields with special requirements for surface roughness, e.g. biosensors [11]. Some researchers tried to make some changes by adjusting the pH value, changing the dopamine concentration, replacing the buffer system, etc., to achieve smoother pDA coatings but with little success [12]. Others chose analog molecules of DA as monomers. Levodopa (L-3,4-dihydroxyphenylalanine, LD) and norepinephrine (NE) are two catecholamine molecules most similar to DA in chemical structure, in which LD has one additional carboxyl group, and NE has one additional hydroxyl group in the ethyl chain when compared with DA, as shown in Fig. 1. As expected, LD and NE, both can self-polymerize to form coatings on various surfaces in an aerobic alkaline buffer system, as DA does [13]. However, there are significant differences between the catecholamine coatings derived from the different monomers. Polymerized NE coatings (pNE) are reported much smoother than pDA, and the dimer of 3,4-dihydroxybenzaldehyde (DHBA) was proved responsible for the suppressed aggregation of pNE particles and the formation of smooth pNE coating, because the simple addition of DHBA to the polymerization system of pDA also resulted in significantly decreased roughness [14]. LD is reported difficult to form a coating as thick as pDA in buffer with low ionic strength, because the intermediate products during polymerization are soluble melanin-like molecules [15] or non-precipitating supramolecular nanoaggregates [16]. Iwasaki et al. found that polystyrene particles modified with different catecholamine coatings, including pDA, pNE, and pLD, showed different structural colors [17].

One of the most important applications of the above-mentioned catecholamine coatings is biomedicine, including surface modification of biomaterials [18], biosensors [19], drug delivery systems [20], tissue engineering [21] or others. However, different application scenarios may have different requirements for the properties of catecholamine coatings. For example, pDA coatings can support the grafting of molecules containing –SH and –NH₂ groups, and the additional –COOH groups of pLD coating are expected to provide further grafting possibilities [22]. Moreover, the –COOH groups make pLD coating more hydrophilic to reduce the non-specific adsorption of proteins [23]. pNE coatings are reported smoother than pDA, thus more suitable for biosensors modification to avoid the interference of pDA nanoparticles on the detection results [24]. Therefore, it is necessary to study and compare the properties of the three above-mentioned coatings more systematically to allow the decision for a specific application. But due to the generally low recognition of the pLD and pNE coatings in the literature, there is little systematic evaluation and comparison of the properties of the three catecholamine coatings. The evaluation here focuses on the application of blood-contacting devices, by comparing the blood compatibility, cytocompatibility, and histocompatibility of the three catecholamine coatings. The most suitable catecholamine coating for the application in the cardiovascular field is determined.

2. Materials and methods

2.1. Materials

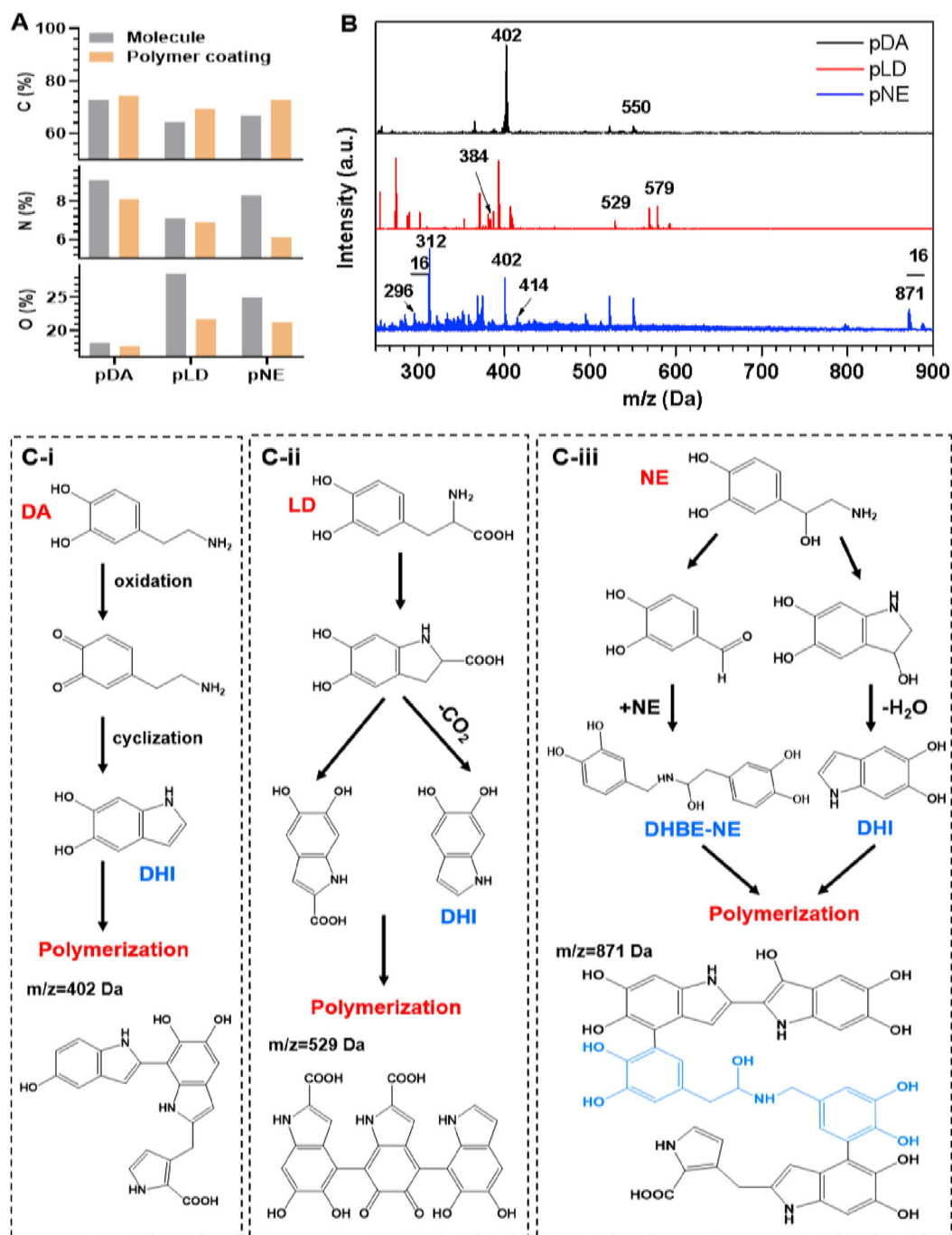DA, LD, and NE were purchased from Sigma Aldrich. Phosphate-

Fig. 2. Chemical composition and atomic rate analysis of pDA, pLD, and pNE coatings. (A) Atomic compositions obtained by XPS of the monomers and derived polymer coatings. (B) MALDI-MS analysis of pDA, pLD, and pNE solid powder. (Ci-iii) Suggested mechanisms of DA, LD, and NE self-polymerization.

buffered solution (PBS) and Tris-HCl buffer solution were obtained from Hyclone Laboratories (Logan, Utah, USA). 316 L stainless steel (316 L SS) substrates (foils, wafers) were processed by Chengdu Derbo Steel Co. Ltd (Sichuan, China). Milli-Q water (18 MΩ, Millipore) was employed in all tests of the study.

2.2. Preparation of the catecholamine coatings

The catecholamines, DA, LD, and NE with the concentration of 1 mg/mL in the Tris-HCl buffer solution (0.01 M, pH 8.5) were distributed on the 316 L SS wafers (Ø10 mm). After 24 h of deposition at 25 °C, the wafers were ultrasonically cleaned in distilled water and dried with nitrogen gas. The obtained samples were labeled as pDA,

pLD and pNE, respectively.

2.3. Physical properties of the catecholamine coatings

Firstly, scanning electron microscopy (SEM, JSM-7800F, Electronics, Japan) was used to analyze the surface morphology of the catecholamine coatings. All the samples were dehydrated, dealcoholized, and dried before analysis. SEM was operated at 2.7 kV × 15 mA under a pressure of 5×10^{-4} Pa. Then the surface roughness of the coatings was measured via atomic force microscopy (AFM, Asylum MFP-3D-BioAFM, Asylum Research, USA) in a noncontact mode with Si cantilevers, in a scanning range of 5 μm × 5 μm. The thickness of the coatings was determined by using a spectroscopic
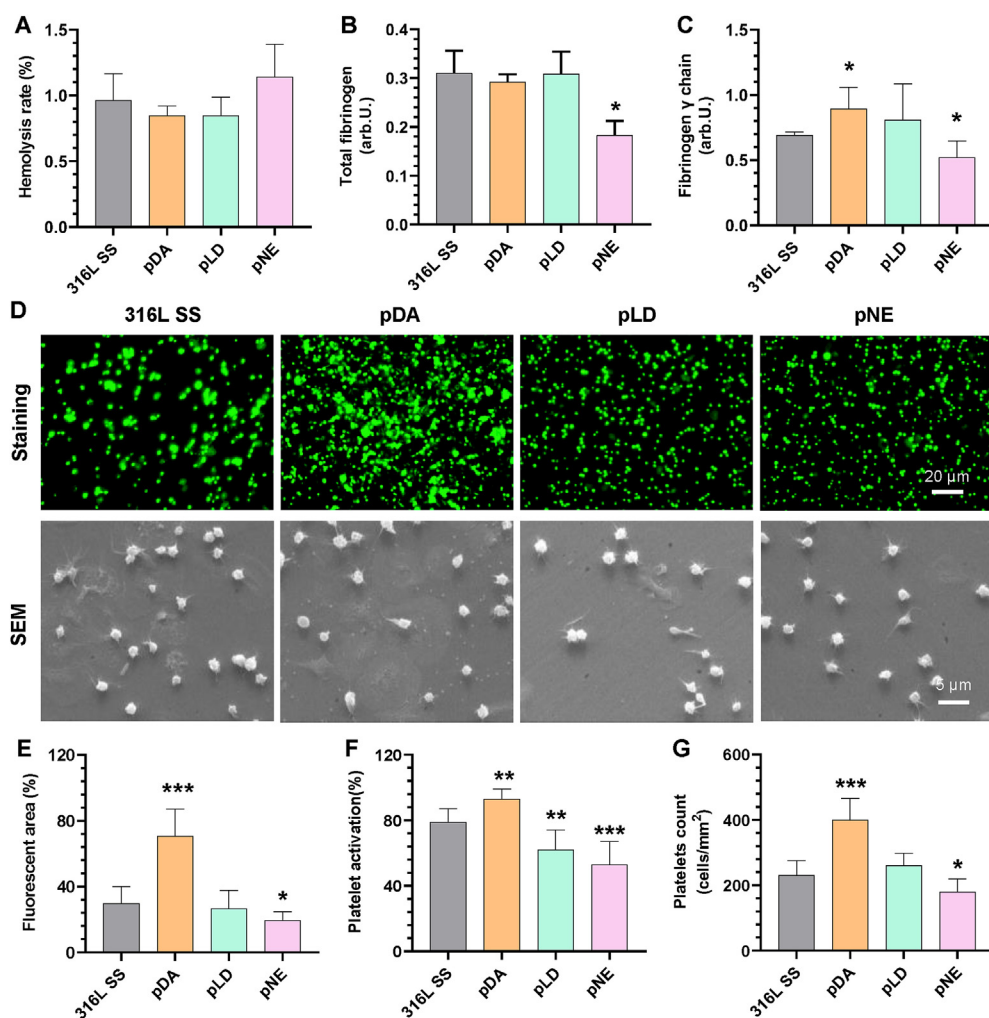
Fig. 3. Hemocompatibility of bare 316 L SS and 316 L SS coated with pDA, pLD, and pNE *in vitro*. (A) Hemolysis rate (%) of red blood cells on different coatings. (B) Adsorbed fibrinogen and (C) their exposure of γ chain on all the samples. (D) Representative fluorescent and SEM images for examining the platelet adhesion and activation. (E) Fluorescent area (%) of adherent and activated platelets. (F) Percentage of activated platelets of the different coating surface. (G) Numbers of the adherent and activated platelets on 316 L SS, pDA, pLD, and pNE samples. Data presented as mean ± SD (n = 6 or n = 12) and analyzed using a one–way ANOVA (*$p < 0.05$, **$p < 0.01$ and ***$p < 0.001$ compared to 316 L SS). (For interpretation of the references to color in this figure legend, the reader is referred to the Web version of this article.)

ellipsometer (M − 2000V, J.A. Woollam, USA) using the Cauchy model. To analyze the water contact angle of the coatings, a Drop Shape Analysis System DSA100 (Krüss, Hamburg, Germany) was used, and the DSA 1.8 software was adopted to process the image of a sessile drop of 5 μL distilled water.

2.4. Chemical properties of the catecholamine coatings

Acid Orange II (AO II, Sigma-Aldrich, USA) was implemented to quantify the surface amino groups of the coatings [25]. Micro BCA protein assay kit was used to quantify the phenolic hydroxyl/quinone groups of the coatings as the following steps. Firstly, 160 μL of BCA solution was added on the surface of the samples, and incubated at 30 °C for 90 min, then the absorbance of 150 μL reaction solution was detected at 562 nm. Infrared absorption spectra of the three coatings were obtained using a Grazing incidence attenuated total reflection Fourier transform infrared spectroscopy (GATR-FTIR) (Nicolet model 5700) in the range of 4000–400 cm^{-1} to analyze their chemical structure. X-ray photoelectron spectroscopy (XPS, K-Alpha, Thermo Electron, USA) was applied to determine their atomic composition. The instrument was operated at 12 kV × 15 mA at a pressure of 3 × 10^{-7} Pa. A wide-scan survey spectrum over a binding energy ranging from 0 to 1400 eV was recorded using the Al Kα excitation at a pass energy of 80 eV for estimation of the chemical elemental composition and 10 eV for high-resolution detailed scans. The system was calibrated using the C1s peak at 284.8 eV. Possible chemical structures of the coatings were determined by the MALDI-TOF MS as reported elsewhere [26].

2.5. Hemocompatibility of the catecholamine coatings

2.5.1. Hemolysis tests

To evaluate the erythrocyte compatibility of the catecholamine coatings, an *in vitro* hemolysis test was performed. About 10 mL of whole blood was collected and added to 8 mL saline solution. All samples were previously immersed in 10 mL of saline in tubes at 37 °C for 30 min. Then, 200 μL of the diluted whole blood was added to the tubes containing the samples and incubated at 37 °C for 1 h. Saline solution (0% hemolysis) was selected as negative control and deionized water (DI water) (100% hemolysis) as the positive control. The incubated whole blood was collected and centrifuged at 3000 rpm for 5 min, and the absorbance of the released hemoglobin from red blood cells was read using a microplate reader (uQuant, Bio-Tek Instruments Inc., USA) at 540 nm. The hemolysis rates were calculated according to the following formula:

$$\% \text{ Hemolysis} = [(A_a − A_c)/(A_b − A_c)] \times 100 \quad (\text{eq. (1)})$$

where A_a refers to the absorbance value of samples, A_b and A_c are the absorbance values of the positive group and negative controls, respectively.

2.5.2. Fibrinogen (Fg) adsorption and denaturation

Fresh human whole blood was obtained from healthy human volunteers and anti-coagulated with 3.2% tri-sodium citrate in a 9:1 volumetric ratio. The whole blood was centrifuged at 3000 rpm for 15 min to prepared platelet-poor plasma (PPP). About 100 μL PPP was added
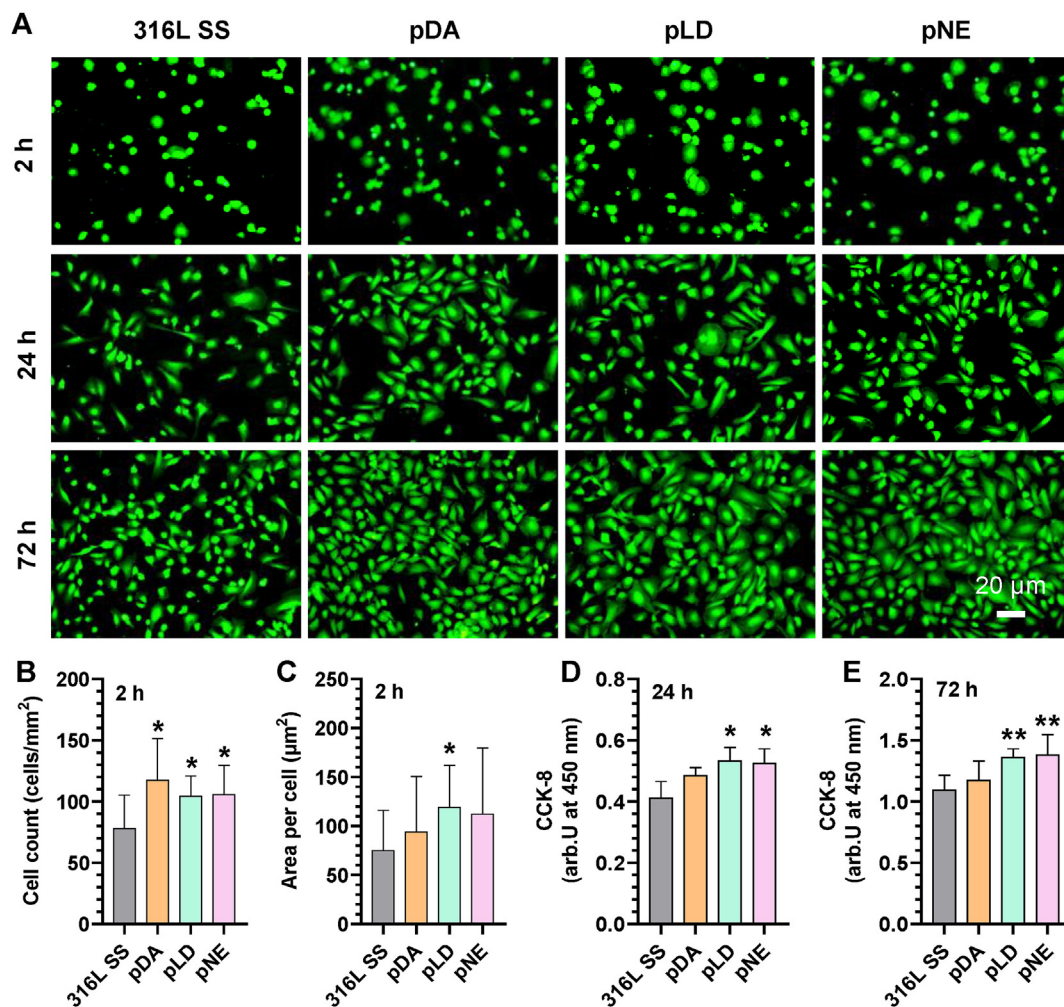
Fig. 4. Adhesion and growth of HUVECs cultured on bare 316 L SS, pDA, pLD, and pNE coatings. (A) Fluorescence staining of ECs cultured on the surfaces for 2, 24, and 72 h. (B) Cell count and (C) area per cell grown on the coating surfaces for 2 h, calculated from at least 12 images. (D) Growth analysis of ECs incubated in cell culture media for 24 and (E) 72 h determined by CCK-8 kit. Data are presented as mean $\pm$ SD (n = 4, or n = 6, or n = 12) and analyzed using a one–way ANOVA, *p < 0.05, **p < 0.01 and ***p < 0.001 compared to 316 L SS.

on each 316 L SS wafer, bare or with catecholamine coating, and incubated at 37 °C for 2 h. The adsorbed and denatured Fg on the above coatings was quantified using the method of ELISA, refer to the detailed description reported by Yang et al. [27].

2.5.3. Platelet adhesion and activation

Fresh human whole blood was centrifuged at 1500 rpm for 15 min to prepare platelet-rich plasma (PRP). 50 μL PRP was added on the surface of each sample and incubated for 30 min at 37 °C. Subsequently, samples were rinsed in 0.9 wt% NaCl solution to remove non-adherent platelets and fixed with 2.5 wt% glutaraldehyde solution. Then, the samples were dehydrated, dealcoholized, and dried, then examined by SEM.

2.6. Cytocompatibility of the catecholamine coatings

2.6.1. Cells isolation and culture

Human umbilical vein endothelial cells (HUVECs) and artery smooth muscle cells (HUASMCs) were isolated from human umbilical cords, according to our previous work [28], and cultured and subcultured in a special medium for ECs (ECM, Sciencell, US) and SMCs (SMCM, Sciencell, US) in a cell incubator with 5% CO_2 at 37 °C. Cells at passage 3 to 9 were used in the experiments. RAW264.7 macrophages were purchased from Zhong Qiao Xin Zhou Biotechnology Co., Ltd

(Shanghai, China) and cultured in DMEM medium (Beit-Haemek, Israel) with high glucose supplemented with 10% fetal bovine serum.

2.6.2. Cell adhesion and proliferation assay

HUVECs, HUASMCs, and RAW264.7 macrophages were seeded onto 316 L SS and catecholamine coatings at a density of 2.0×10^4 cells/well of 24-well cell culture plate, respectively. After 2, 24, and 72 h of incubation, the cells were fixed, stained by rhodamine123, and inspected by using a fluorescence microscope (DMRX, Leica, Germany). After 24 and 72 h of culture, cell viability was detected via Cell Counting Kit-8 (CCK-8, Dojindo, Japan).

2.7. Histocompatibility of the catecholamine coatings

2.7.1. Expression of inflammatory cytokines by macrophages

After 24 h of incubation, the supernatant of the macrophages grown on the bare and coated 316 L SS samples were collected, 6 inflammatory cytokines secreted by macrophages were detected by using BioLegend's LEGENDplex™ multiplex assay kit based on flow cytometry, including 3 pro-inflammatory cytokines (IL-6, TNF-α, IL-1β)and 3 anti-inflammatory cytokines (TGF-β1, IL-23, and IL-10).

2.7.2. Subcutaneous implantation experiment

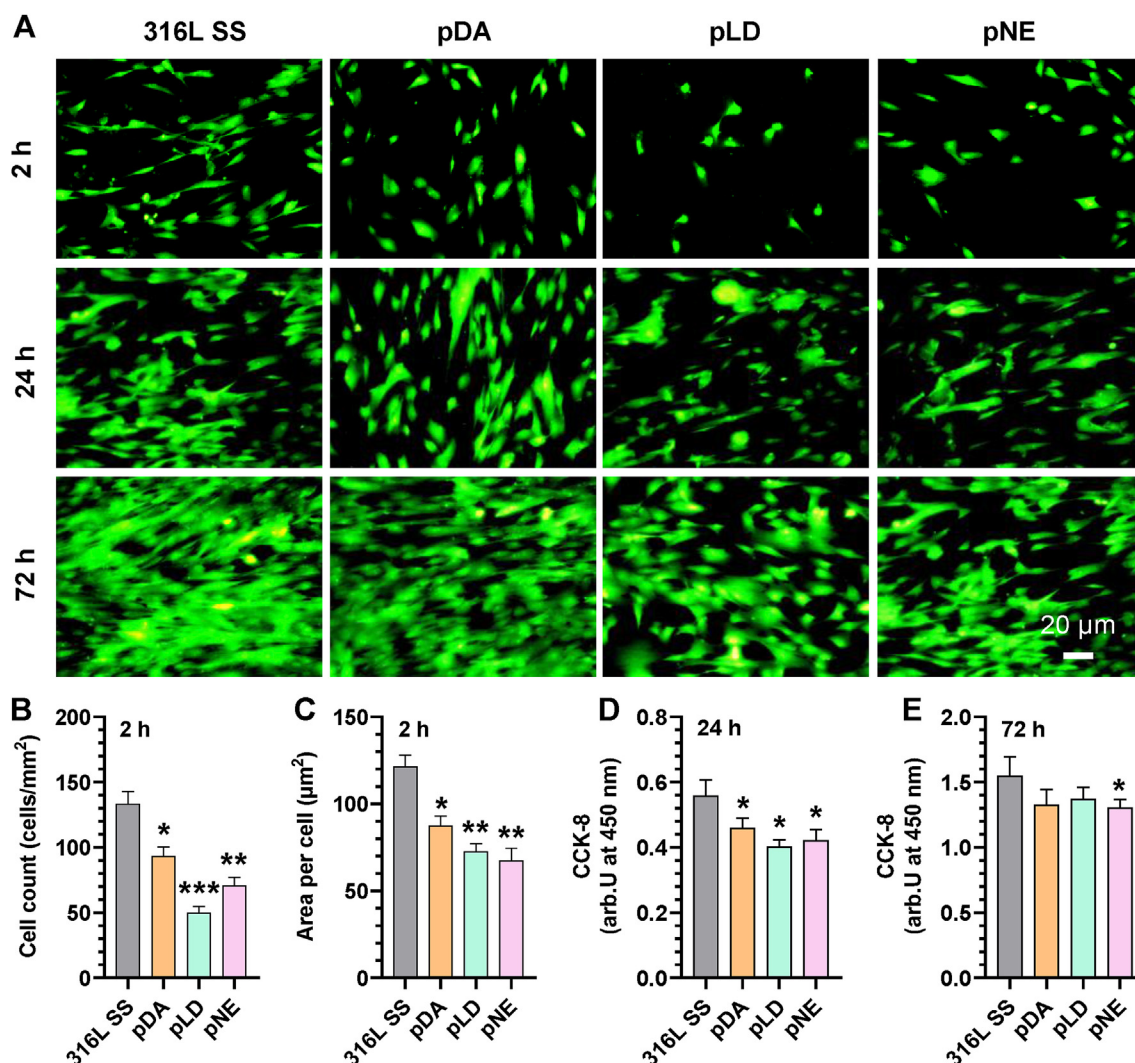Under the compliance with the agreements of animal ethics and the

Fig. 5. Adhesion and proliferation of HUASMCs on bare 316 L SS and 316 L SS modified with pDA, pLD, and pNE coatings. (A) Fluorescent images of SMCs on the 316 L SS, pDA, pLD, and pNE samples after culture for 2, 24, 72 h stained by Rhodamine123. (B) Cell count and (C) area per cell grown on the coating surfaces for 2 h, determined from at least twelve images. (D) The proliferation of SMCs after culture for 24 and (E) 72 h determined by CCK-8 assay. Data presented as mean ± SD (n = 4, or n = 6, or n = 12) and analyzed using a one–way ANOVA, *p < 0.05, **p < 0.01 and ***p < 0.001 compared to 316 L SS.

protocols of animals' use, experiments on animals were performed to evaluate the anti-inflammatory property of the different coatings. Twelve male SD-rats with the weight of 150–200 g and four groups of specimens of coatings were used in these studies. The samples of 316 L stainless steel with a major axis of 5 mm and a minor axis of 2 mm were ultrasonically cleaned before use. All the rats were fed adaptively for 1 week. Fifteen days after specimen implantation, the samples and the covered tissue were collected and fixed with 4% paraformaldehyde for further hematoxylin-eosin staining analysis.

2.8. Statistical analyses

All experimental data were presented as mean ± standard deviations (n = 6 or n = 12), and the groups were compared for significant differences using a one-way ANOVA with statistical software (SPSS, Armonk, New York, USA). The value of P < 0.05 was considered statistically significant.

3. Results and discussions

3.1. Preparation and characterization of pDA, pLD, pNE coatings

The catecholamines DA, LD, and NE have high similarity in their chemical structures. As shown in Fig. 1A, LD has one additional –COOH, and NE has one additional –OH group in the ethylamine chain compared to DA. The molecules were gradually oxidized in Tris buffer when exposed to air over time, to generate products with the color from light brown to black. DA changed the color fastest, LD was the second, and NE was the slowest (Fig. 1B). After 24 h of incubation, an obvious brown pDA coating and a light brown pNE coating was constructed on stainless steel wafers, but pLD did not form an obvious coating (Fig. 1C). The coating thickness was measured by ellipsometry (Fig. 1D) and correlated with the color shade of the coatings. In consistence with other reports [29], LD hardly forms a thick coating under normal ionic strength, because of the soluble melanin-like intermediate products or non-precipitating supramolecular nanoaggregates [30]. Moreover, the pLD coating did not seem to completely cover the substrate, which can be deduced from the presence of the iron atom in XPS spectra from the substrate (Fig. 1E). The main reactive functional groups of the three coatings, namely amino (-NH$_2$) and phenolic hydroxyl (Ph-OH), was
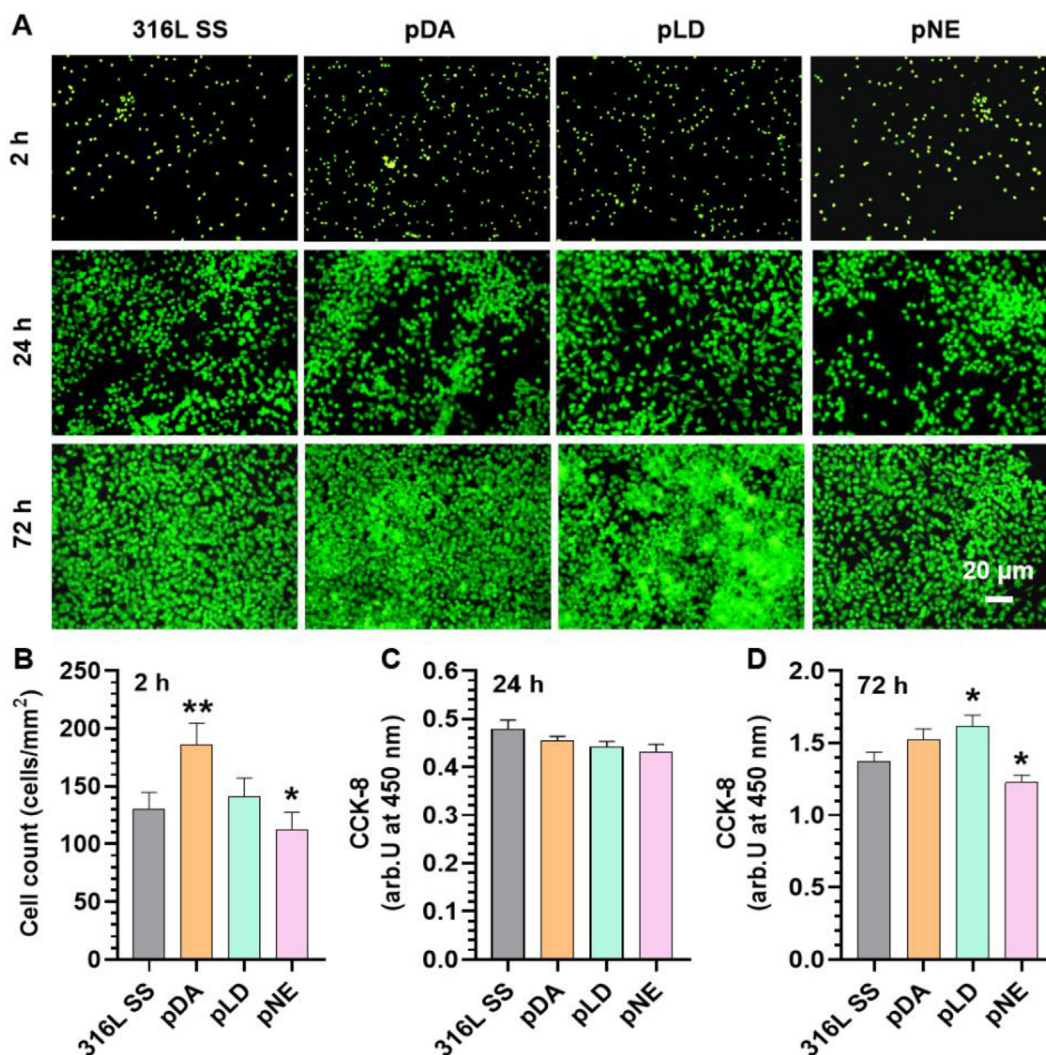
Fig. 6. Adhesion and growth of macrophages on bare 316 L SS and 316 L SS modified with pDA, pLD, and pNE coatings. (A) Fluorescent staining images of macrophages on the 316 L SS, pDA, pLD, and pNE samples after culture for 2, 24, and 72 h. (B) Cell count of macrophages on coatings based on at least twelve images. (C) Growth of macrophages for the culture of 24 and (D) 72 h using CCK-8. Data presented as mean $\pm$ SD (n = 6) and analyzed using a one–way ANOVA, *p $<$ 0.05, **p $<$ 0.01 and ***p $<$ 0.001 compared to 316 L SS.

characterized by AO II and Micro-BCA assay, and the results are shown in Fig. 1F&G. The pDA coating had the largest density of –NH$_2$ and Ph-OH groups, while the pLD coating had the lowest. In Fig. 1H, average water contact angles were shown. The mirror-polished 316 L SS surface had a water contact angle of 58 $\pm$ 5°, pDA-coating had 45 $\pm$ 2°, and pLD and pNE-coated 316 L SS had 29 $\pm$ 2° and 38 $\pm$ 3°, respectively (Fig. 1D&S3). Surface modification of 316 L SS by the three catecholamine coatings significantly decreased the water contact angles, thanks to the hydrophilic functional groups, such as –NH$_2$ and Ph-OH. The pLD coating was the most hydrophilic, which was consistent with the results of others, and the hydrophilic –COOH group was reported to play an important role [31].

3.2. Chemical composition analysis of pDA, pLD, and pNE coatings

To further understand the formation mechanism of these three coatings, analyses of FTIR, XPS, and MALDI-MS were performed to detect the oxidation pathways in this study. The characteristic peaks of the FTIR data in 3300–3400 cm^{-1} (-OH, stretching absorption) and 1510 and 1619 cm^{-1} (-Ph, absorption) indicated that the main structure of these three coatings was the catechol unit (Fig. S4). The surface chemical composition and atomic rates of pDA, pLD, pNE coating were

further analyzed quantitatively by XPS (Fig. 2A&S5). The high-resolution spectra of C 1s, N 1s, O 1s were further curve-fitted for functional group analysis (Fig. S6). The peak positions and atomic concentrations of the functional groups are listed in Table S1. The atomic concentration of each functional group was obtained by multiplying the percentage of the functional group obtained from the curve fitting by the atomic concentration of the element. As a very sensitive surface technology, MALDI-MS was employed to analyze more structural compositions, such as the polymerization (Fig. 2B&S7).

The polymerization of the dopamine molecules to the pDA coating did not alter the atomic composition (C, N, O) of the pDA coating significantly compared with the theoretical value of the DA molecule, which is consistent with previous reports. These results were also confirmed by the MALDI spectra peaks around m/z 402 and 550 Da, corresponding to the compounds in Fig. 2C-i&S7. However, the oxygen ratio (O%) of LD and NE molecules and the nitrogen ratio (N%) of NE molecule dropped significantly after polymerization to the pLD and pNE coatings (the O% dropped from 28.6% to 21.7% and from 25% to 21% in pLD and pNE, respectively; the N% dropped from 8.2% to 6.1% in pNE) (Fig. 2A). Combined with the MALDI-MS peaks around m/z 384, 529 and 579 Da, we assume that the significant decrease in the O ratio of pLD coating was caused by the LD oxidation and loss of a
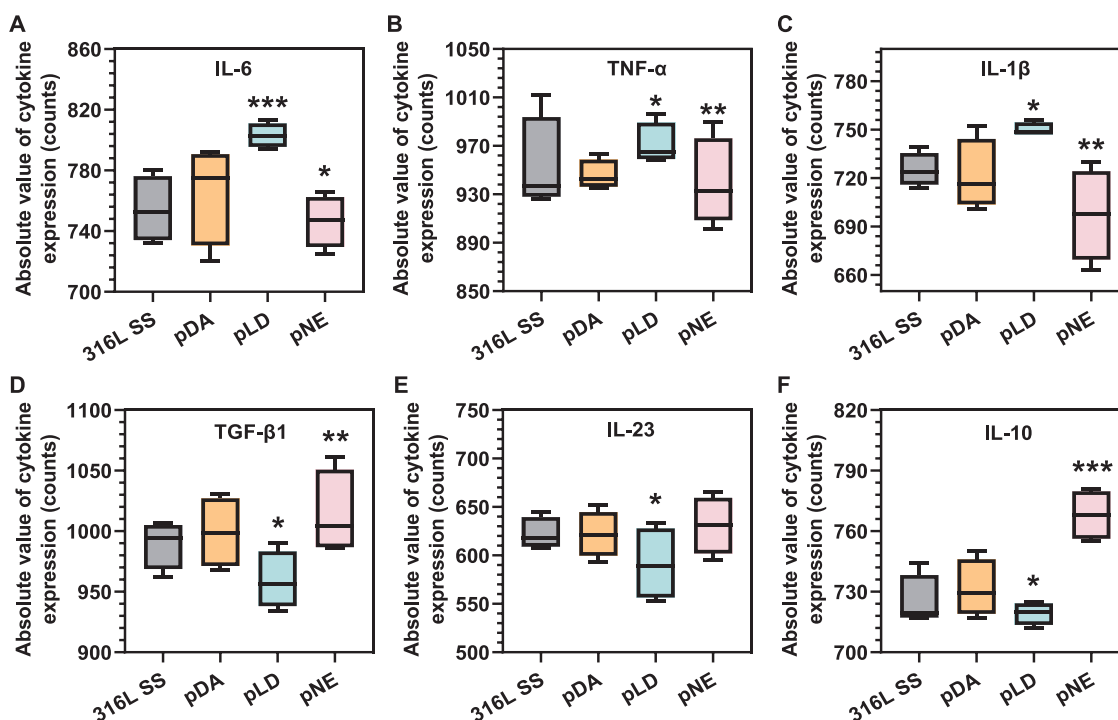
Fig. 7. Absolute value of macrophages cytokine expression of inflammatory markers M1 and anti-inflammatory markers M2 determined by a multiplex assay using flow cytometry with 10 μL cell culture medium, 5000 cells were counted for each group. (A–F) The value of cytokine expression of IL-6, TNF-α, IL-1β, TGF-β1, IL-23, and IL-10. Data presented as mean ± SD (n = 6) and analyzed using a one–way ANOVA, *p < 0.05, **p < 0.01 and ***p < 0.001 compared to 316 L SS.

carbon dioxide to form 5,6-dihydroxyindole (DHI) (Fig. 2C–ii) which commonly forms during pDA, pLD, pNE polymerization [20]. The O 1s high-resolution spectrum of pLD coating shows that there are still many carboxyl groups, which indicate that pLD coating was formed by the polymerization of DHI and multiple intermediate products. This explains the low water contact angle of the pLD coating.

The significant reduction of the N ratio in the pNE coating may be caused by tautomerization and non-methanogenic breakdown reaction to form the new intermediate 3,4-dihydroxybenzaldehyde (DHBA). The dropped O ratio in pNE coating indicates that DHBA and NE probably further polymerized by Schiff base reaction (Fig. 2C–iii). The C 1s high-resolution spectra show that C–OH, C–NH- groups at 286.2 eV in pNE coating were significantly higher than in pDA and pLD. These results indicate that the pNE coating was formed by the polymerization of DHBA-NE, DHI, and their intermediate products. MALDI-MS peaks at 296, 312, 402, 414, 871, and 887 Da corresponding to the structures in Fig. 2C–iii&S7B further confirm these results.

The N 1s spectra of the three coatings were fitted with three peaks assigned to -C-NH at 400.3 eV, aromatic N at 399.5 eV, and C–NH$_3^+$ at 402.0 eV. The major contribution to N 1s came from -C-NH, not from the other two components (aromatic N and C–NH$_3^+$). This implies that the cyclization reaction occurs during pDA, pLD, pNE formation, leaving some residual open-chain units on these coatings.

3.3. Hemocompatibility evaluation of pDA, pLD, pNE coating in vitro

Catecholamine coatings have been widely used for surface modification of blood-contacting materials and implants [32]. When the coatings come into contact with blood, they usually face plasma protein adsorption and denaturation, platelet adhesion and activation or induction of hemolysis, etc [33], which may eventually trigger thrombus formation [34]. DA, LD, and NE are important transmitters or their precursors in the human body, their polymerized coatings are theoretically safe because the content of free monomer molecules in the coating is relatively low.

All polymers induced less hemolysis compared to 316 L SS, one of

the most widely used biomaterials (Fig. 3A). However, both the plasma protein adsorption and activation, and the platelet adhesion and activation significantly differed between the three coatings. Only the pNE coating significantly reduced the adsorption and activation of Fg compared to 316 L SS, as shown in Fig. 3B&C. Platelet adhesion and activation were determined from the fluorescent photographs and SEM images by analysis of the platelet expansion and collapse of the structure (Fig. 3D). They indicate that the pDA coating resulted in a significant increase in platelet adhesion and more severe activation than the other coatings. The pNE coating showed the best hemocompatibility, with the least platelet adhesion and activation (Fig. 3E, F&G), and most of the platelets were round with only a few filamentous pseudopodia protruding.

Wettability, surface functional groups, and topography, among others, are important parameters for the hemocompatibility of a material [35]. Specifically, hydrophilic surfaces show low interaction with proteins and cells. For example, hydrophobic –CH$_3$ surfaces induced more Fn adsorption and platelet adhesion than hydrophilic –COOH [36]. The surface charge is an important factor affecting the protein adsorption and platelet adhesion, and positively charged surfaces were reported to enhance platelet activation through factor VII activating protease [37]. Microscaled surfaces cause more protein adsorption than nano-scaled surfaces, and the amount of protein adsorption on surfaces with the same dimension is related to the effective surface area [38]. Therefore, the pDA coating, with the highest water contact angle and the largest amount of positively charged –NH$_2$ groups among the three coatings, resulted in the largest amount of Fg adsorption and activation, and induced more adhesion and stronger activation of platelets. However, blood compatibility of the pLD coating, with the lowest water contact angle and the smallest amount of positively charged –NH$_2$, and with additional negatively charged –COOH, was not better than the pNE coatings. The probable interpretation is that the pLD coating did not cover the base material completely, and the exposed 316 L SS induced protein and platelet adhesion and activation.
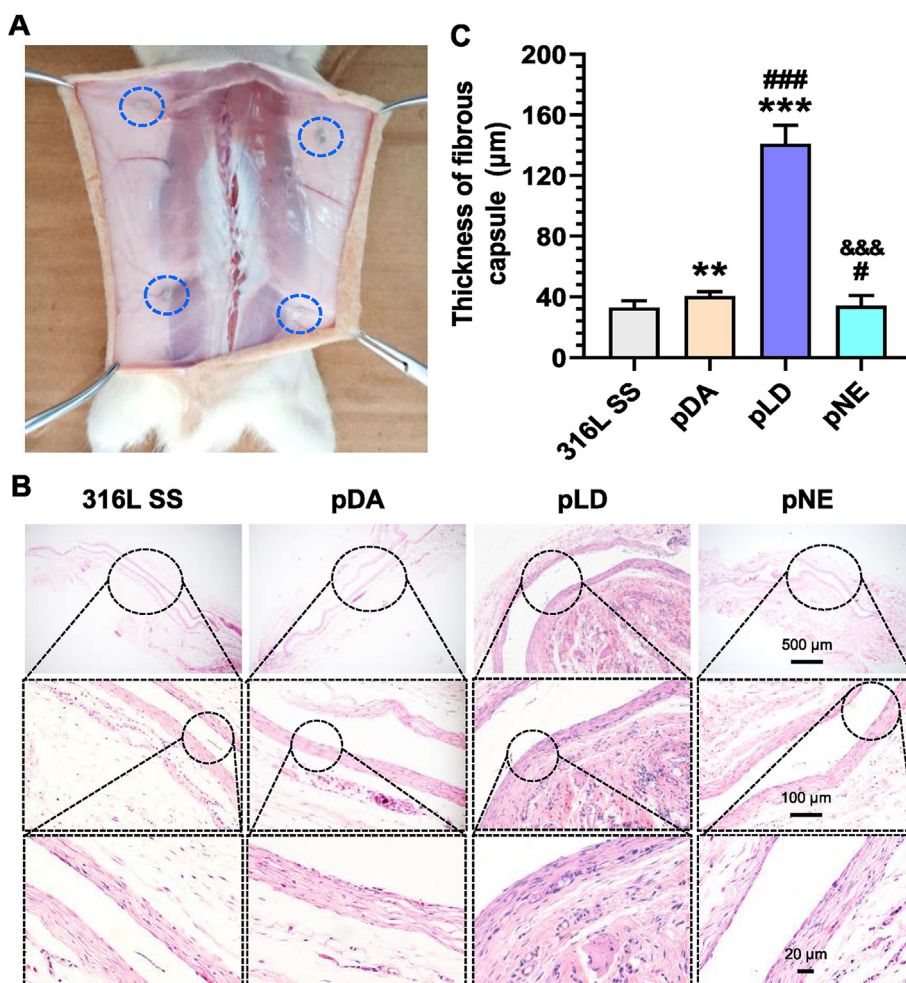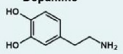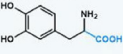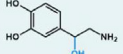
Fig. 8. Histocompatibility evaluation of bare 316 L SS and 316 L SS modified with pDA, pLD, pNE coatings by subcutaneous implantation in male Sprague Dawley rats for 2 weeks. (A) Photo before subcutaneous sampling; (B) Micrographs of the hematoxylin and eosin (HE) stained tissue adjacent to samples; (C) Thickness of fibrous capsules around the samples. Data presented as mean $\pm$ SD (n = 6) and analyzed using a one–way ANOVA (**p < 0.01 and ***p < 0.001 compared to 316 L SS; #p < 0.05 and ###p < 0.001 compared to pDA; &&&p < 0.001 compared to pLD).

Table 1
Summary of the hemocompatibility, cytocompatibility, and histocompatibility of the three catecholamine coatings.

Monomer	Coating	Functional group	Platelet adhesion and activation	HUVECs growth	HUASMCs growth	Inflammatory response
Dopamine	pDA	H	H	L	H	M
Levodopa	pLD	L	M	M	M	H
Norepinephrine	pNE	M	L	H	L	L

(H: high; M: medium; L: low)

3.4. Adhesion and growth behavior of HUVECs and HUASMCs

As catecholamine coatings are increasingly used to modify cardiovascular devices (e.g. stents or vascular grafts), it is necessary to compare the reaction of vascular cells to the different catecholamine coatings. Abnormal growth of ECs and SMCs on vascular stents, such as ECs

inhibition and SMCs hyperplasia, lead to complications such as in-stent restenosis (ISR) and late thrombosis (LT), finally resulting in stent failure, which has to be avoided [39].

Firstly, we incubated HUVECs on the pDA, pLD, and pNE coatings. The results of immunofluorescent staining showed that HUVECs adhered and grew well on the bare and modified 316 L SS with

catecholamine coatings (Fig. 4A). Quantitative results of cell number, cell area, and cell viability are shown in Fig. 4B to G. After 2 h of incubation, a significantly larger amount of HUVECs adhered to the three coatings compared to bare 316 L SS (Fig. 4B), and the adherent cells spread to a higher degree, especially on the pLD coating (Fig. 4C). The proliferation and viability of HUVECs were determined by the CCK-8 kit after incubation for 24 h and 72 h. As shown in Fig. 4D&E, the proliferation and viability of HUVECs on the pDA coating tended to be higher than on 316 L SS, but with no statistical significance. However, those on the pLD and pNE coatings were significantly higher compared to 316 L SS.

The adhesion and proliferation behaviors of HUASMCs on the different catecholamine coatings also were investigated. As shown in Fig. 5A, all of the coatings showed a significant inhibitory effect on SMC adhesion after incubation for 2 h when compared with the bare 316 L SS (Fig. 5B&C). The cell viability of SMCs after 24 h of incubation further demonstrated significant inhibition of the growth of SMCs by catecholamine coatings, which was consistent with some other studies [40], but there was no remarkable difference between coatings (Fig. 5D). However, the inhibitory effect of pDA and pLD coatings became not obvious after 72 h of incubation, except for pNE (Fig. 5E).

In the surface modification of biomaterials, the pDA is one of the most widely studied coatings, and its effect on the growth behavior of many kinds of cells has been deeply studied. Usually, the pDA coating can promote cell adhesion and proliferation in most cases [41,42], but the response of different cells to the coating is different. For example, Lee et al. have reported that a pDA coated surface supports the adhesion of fibroblasts while it limits the adhesion of megakaryocytes [1]. Yang et al. reported that the pDA coating promotes the growth of ECs but inhibits SMCs [43]. In this study, different catecholamine coatings had comparable promoting effects on ECs, but slightly different inhibitory effects on SMCs. Only the inhibitory effect of the pNE coating on SMCs did persist for 72 h. The selectivity of vascular cells of catecholamine has been confirmed in some other articles [40], that is, it selectively promotes the growth of ECs and inhibits the growth of SMCs. However, the mechanism of vascular cell selectivity of catecholamine coatings has not been reported.

The factors affecting cell adhesion and growth on biomaterials usually include 1) The amount and type of protein adsorbed on the material [44]. Fibronectin (FN) is thought to promote the adhesion and growth of most cells, because its reaction site, integrin $\alpha_5\beta_1$, is widely expressed in many types of cell. 2) Some properties of the material itself. Surface functional groups, for example, can directly interact with the integrins on the cell surface, affecting cell adhesion and growth. The incorporation of -NH2 group into plasma-polymerized pyrrole (PPPy) structure, was very favorable to establish hydrogen bonds with Asn224 and/or Asp227 residues, part of the integrin $\alpha_5\beta_1$ pocket [45]. Wang et al. reported that improved growth of ECs by pDA coating was related to the binding of FN to integrin $\alpha_5\beta_1$ [46]. 3) Integrins on the cell surface. Even on the same material, the growth behavior of different cells may differ significantly. For example, the growth of ECs on the surface of LN or REDV (Arg-Glu-Asp-Val) peptide was significantly promoted, while that of SMCs was not. The different expression of integrin $\alpha_4\beta_1$ was demonstrated responsible for the different cell growth behavior [47]. We speculate that the difference in growth behavior of ECs and SMCs on catecholamine coatings may also be related to integrin, but systematic molecular biology studies are needed to determine which integrin plays a key role.

3.5. Adhesion, growth, and phenotype of macrophages

When cardiovascular materials or implants come into contact with blood or vascular tissue, except for the above-mentioned blood and vascular cells, their influence on immune cells is also inevitable. Macrophages are important immune cells at the interface of innate and adaptive immune systems, and they also play an important role in

wound repair. Considering vascular stent implantation, M1 macrophages are involved in the early inflammatory response to vascular tissue injury caused by stent implantation, and M2 macrophages are involved in late tissue repair [48]. Therefore, we investigated the effects of pDA, pLD, and pNE coatings on the adhesion, proliferation, and the phenotype of macrophages (Fig. 6 and Fig. 7). After 2 h of incubation, the most macrophages adhered to the pDA coating, whereas the least macrophages adhered to the pNE coating (Fig. 6A&B). After 72 h of incubation, the number of macrophages on the pNE coating remained the least, and the largest number of macrophages was on the pLD coating (Fig. 6D) and in a higher degree of aggregation (Fig. 6A).

Furthermore, we studied the phenotype of macrophages on the different coatings (including M1 and M2 phenotype), which are characterized by different inflammatory cytokine expressions. M1 macrophages express more pro-inflammatory factors IL-6, TNF-α, or IL-1β, whereas M2 macrophages express more anti-inflammatory factors TGF-β1, IL-23, or IL-10 [49–51]. These cytokines were determined using a multiplex assay in the supernatants of Raw264.7 macrophages seeded on the 316 L SS, pDA, pLD, and pNE coatings. In general, macrophages grown on the pLD coating expressed significantly higher amounts of pro-inflammatory factors (TNF-α and IL-1β) but lower amounts of anti-inflammatory factors (TGF-β1, IL-23, and IL-10), while on pNE, macrophages expressed significantly less pro-inflammatory factors (IL-6, TNF-α, and IL-1β) but more anti-inflammatory factors (TGF-β1 and IL-10), as shown in Fig. 7. This indicates that the pLD coating may trigger more inflammatory reaction than the other two catecholamine coatings, and the pNE coating may have the best histocompatibility.

It is well known that the microenvironmental cues of a biomaterial play a key role in modulating the response of macrophages, including 1) physical properties such as stiffness, topography, and wettability et al., 2) chemical properties including surface functional groups and the release of active molecules [52]. Comparing the microenvironmental cues of the three above catecholamine coatings, we found that the pNE coating was the smoothest. However, according to Chen et al. macrophages are insensitive to topography changes below 500 nm [53], thus the roughness may not be the main factor influencing the behavior of macrophages. Hotchkiss et al. found that titanium surfaces with high wettability provide an anti-inflammatory microenvironment [54], but the most hydrophilic catecholamine coating in this study, pLD, triggered the strongest pro-inflammatory reaction, so there must be further cues that play a more important role than the wettability.

The surface functional groups would be the most important differences among the three coatings. pLD contained a certain amount of carboxyl groups, while pNE contained hydroxyl groups. Akilbekova et al. demonstrated that macrophages activated by lipopolysaccharide (LPS) expressed higher TNF-α but lower IL-10 amounts when contacted with the polystyrene (PS) beads with carboxyl surface than those with amino and hydroxyl surfaces [55]. This was consistent with the results of this study, indicating that functional groups on the surface of the coating may be the dominant factor influencing the phenotype of macrophages.

3.6. Histocompatibility of pDA, pLD, pNE coating in vivo

When a medical device is implanted into the body, the surgical injury during implantation and the stimulation of the implanted material or device itself inevitably causes different degrees of foreign body reaction. In the early stage of implantation, the implanted material is surrounded by granulation tissue with varying degrees of an inflammatory reaction, depending on the histocompatibility of the implanted materials themselves. The infiltrating inflammatory cells are mainly neutrophils and macrophages, a small number of plasma cells and lymphocytes. Over time, the granulation tissue gradually matures, forming a fibrous capsule around the devices, thus separating it from the surrounding tissue [56]. The histocompatibility of the implanted biomaterial or medical device can be judged by the thickness of the

fibrous capsule and the amount of infiltrated inflammatory cells. A thinner fibrous capsule and less infiltrating inflammatory cells indicate better histocompatibility.

Bare 316 L SS and catecholamine coated disks were implanted subcutaneously in SD rats. Two weeks after subcutaneous implantation, the skin was opened and the samples were exposed. The color of subcutaneous tissue was normal, and there was no obvious hyperemia, edema, and hardening. All the samples were covered with fibrous capsules, and there was no obvious adhesion with the surrounding tissue, as shown in Fig. 8A. Micrographs of the HE stained tissue adjacent to the samples in Fig. 8B further demonstrated that all the samples were covered with fibrous capsules, accompanied by neovascularization, and the boundaries between the fibrous capsules and the surrounding tissues were clear. However, inflammatory cells were infiltrating the interface between the sample and the fibrous capsule, and between the capsule and the surrounding tissue. Most of them were macrophages, a relatively small number of plasma cells, and occasional lymphocytes. 316 L SS group and pNE group showed less-intense inflammatory cell infiltration than pDA and pLD, indicating a lower level of inflammatory reaction for pNE than for pDA and pLD. Finally, the average thickness of fibrous capsules around the sample, measured from the histological images (Fig. 8C), demonstrated that among the four groups, was thickest for pLD and thinnest for pNE. The difference was statistically significant, indicating that pNE had better histocompatibility.

To sum up, surface modification is still one of the most important techniques in the design and preparation of biomaterials. It endows the materials with different properties for specific application scenarios, such as superhydrophobicity to reduce the adhesion of blood components to cardiopulmonary bypass catheters or inferior vena cava filters, anti-coagulant and anti-hyperplasia properties for vascular stents and grafts et al. [57]. The pDA coating, firstly introduced by Lee et al. has become the most popular intermediate layer for the surface modification of biomaterials, because of its versatility, simplicity, firm binding with the substrate material, and secondary reactivity [58]. Based on the pDA coating, some researchers constructed an antibacterial surface [59], Wang et al. prepared an osteogenic differentiation enhancing material [60], Yang et al. designed an endothelium-mimicking coating for vascular stents [61]. However, there are still some limitations to pDA coatings. For example, molecules that can be grafted on pDA coatings usually must contain $-NH_2$ or $-SH$ groups; the high roughness of pDA may limit its application in biosensors or batteries. NE and LD are structurally related to DA, and also have the ability of self-polymerization to form coatings. However, the different functional groups on the ethyl chain led to different self-polymerization processes, and eventually different coating properties. pLD coating was reported to be more hydrophilic, and pNE coating was demonstrated smoother than pDA coating. But so far, the performance of these three coatings concerning hemocompatibility, cytocompatibility, and histocompatibility had not been explored systematically yet, which was the topic of this study, and the results were summarized in Table 1.

This indicates that the pNE coating may be a better choice for the surface modification of cardiovascular materials, especially vascular stents and grafts. Although it is rarely applied in this field, it deserves to be considered more frequently. The slow formation rate, incomplete substrate coverage, and pro-inflammatory property are the problems that must be overcome in the application of pLD coating. Besides, the pDA coating induced the largest amount of platelet adhesion and the highest platelet activation. Thus, when it was used to modify a blood-contacting material, such as a vascular stent and graft, grafting of anti-coagulant molecules is necessary, such as heparin [62,63] or NO release systems [64].

4. Conclusions

We systematically studied the physical, chemical, and biological performance of three catecholamine coatings, namely poly-dopamine (pDA), poly-levodopa (pLD), and poly-norepinephrine (pNE).

5. pLD was difficult to form a defect-free coating and induced serious inflammatory response, which may limit its application in the modification of biomaterials.
6. pDA has a high number of reactive groups on the surface, which is beneficial for grafting of biomolecules but also resulted in a larger amount of platelet adhesion and more serious platelet activation. Anti-coagulation modification must be adopted when the pDA coating is used for blood-contacting implants.
7. pNE coating had the best hemocompatibility and histocompatibility, and the strongest vascular cells selectivity, making it a better choice for the surface modification of cardiovascular materials, especially for vascular stents and grafts.

CRediT authorship contribution statement

Xing Tan: Writing - original draft, Investigation. **Peng Gao:** Writing - original draft, Investigation. **Yalong Li:** Investigation. **Pengkai Qi:** Conceptualization. **Jingxia Liu:** Validation, Supervision. **Ru Shen:** Visualization. **Lianghui Wang:** Methodology. **Nan Huang:** Supervision, Conceptualization. **Kaiqin Xiong:** Writing - review & editing, Supervision. **Wenjie Tian:** Supervision, Funding acquisition. **Qiufen Tu:** Writing - review & editing, Funding acquisition, Supervision.

Declaration of competing interest

The authors declare no competing financial interest of the manuscript entitled "Poly-dopamine, poly-levodopa, and poly-norepinephrine coatings: Comparison of physico-chemical and biological properties with focus on the application for blood-contacting devices".

Acknowledgements

Appendix A. Supplementary data

Supplementary data to this article can be found online at https://doi.org/10.1016/j.bioactmat.2020.06.024.

References

[1] H. Lee, S.M. Dellatore, W.M. Miller, P.B. Messersmith, Mussel-inspired surface chemistry for multifunctional coatings, Science 318 (5849) (2007) 426–430.
[2] B.D. McCloskey, H.B. Park, H. Ju, B.W. Rowe, D.J. Miller, B.J. Chun, K. Kin, B.D. Freeman, Influence of polydopamine deposition conditions on pure water flux and foulant adhesion resistance of reverse osmosis, ultrafiltration, and micro-filtration membranes, Polymer 51 (15) (2010) 3472–3485.
[3] J. Jiang, L. Zhu, L. Zhu, B. Zhu, Y. Xu, Surface characteristics of a self-polymerized dopamine coating deposited on hydrophobic polymer films, Langmuir 27 (23) (2011) 14180–14187.
[4] H. Meng, Y. Liu, M. Cencer, B. Lee, Adhesives and coatings inspired by mussel adhesive proteins: adhesives and coatings inspired by mussel adhesive proteins, Bioadhe. Biomim: From Nature to Applications (2015) 131–166.
[5] Y.T. Li, M.R. Liao, J. Zhou, Catechol–cation adhesion on silica surfaces: molecular dynamics simulations, Phys. Chem. Chem. Phys. 19 (43) (2017) 29222–29231.
[6] T. Posati, C. Ferroni, A. Aluigi, A. Guerrini, F. Rossi, F. Tatini, F. Ratto, E. Marras, M.B. Gariboldi, A. Sagnella, G. Ruani, R. Zamboni, G. Varchi, G. Sotgiu, Mild and effective polymerization of dopamine on Keratin films for innovative photo-activable and biocompatible coated materials, Macromol. Mater. Eng. 303 (2018) 1700653.
[7] V. Ball, J.Ô. Bour, M. Michel, Step-by-step deposition of synthetic dopamine-

eumelanin and metal cations, J. Colloid Interface Sci. 405 (2013) 331–335.

[8] W.B. Tsai, W.T. Chen, H.W. Chien, W.H. Kuo, M.J. Wang, Poly(dopamine) coating to biodegradable polymers for bone tissue engineering, J. Biomater. Appl. 28 (6) (2014) 837–848.

[9] C.G. Qian, S. Zhu, P.J. Feng, Y.L. Chen, J.C. Yu, X. Tang, Y. Liu, Q.D. Shen, Conjugated polymer nanoparticles for fluorescence imaging and sensing of neurotransmitter dopamine in living cells and the brains of Zebrafish Larvae, ACS Appl. Mater. Interfaces 7 (33) (2015) 18581–18589.

[10] J. Park, T.F. Brust, H.J. Lee, S.C. Lee, V.J. Watts, Y. Yeo, Polydopamine-based simple and versatile surface modification of polymeric nano drug carriers, ACS Nano 8 (4) (2014) 3347–3356.

[11] S.C. Goh, Y. Luan, X. Wang, H. Du, C. Chau, H.E. Schellhorn, J.L. Brash, H. Chen, Q. Fang, Polydopamine–polyethylene glycol–albumin antifouling coatings on multiple substrates, J. Mater. Chem. B. 6 (2018) 940–949.

[12] R. Lakshminarayanan, S. Madhavi, C.P.C. Sim, Oxidative polymerization of dopamine: a high-definition multifunctional coatings for electrospun nanofibers - an overview, in: S.C. Yenisetti (Ed.), Dopamine - Health and Disease, IntechOpen, 2018, pp. 113–132.

[13] Y. Liu, K. Ai, L. Lu, Polydopamine and its derivative materials: synthesis and promising applications in energy, environmental, and biomedical fields, Chem. Rev. 114 (9) (2014) 5057–5115.

[14] Y.H. Ding, L.T. Weng, M. Yang, Z.L. Yang, X. Lu, N. Huang, Y. Leng, Insights into aggregation/deposition and structure of polydopamine film, Langmuir : ACS J. Surf. colloids. 30 (2014) 12258–12269.

[15] S. Moulay, Dopa/catechol-tethered polymers: bioadhesives and biomimetic adhesive materials, Polym. Rev. 54 (3) (2014) 436–513.

[16] F. Solano, Melanin and melanin-related polymers as materials with biomedical and biotechnological applications—cuttlefish ink and mussel foot proteins as inspired biomolecules, Int. J. Mol. Sci. 18 (7) (2017) 1561.

[17] T. Iwasaki, Y. Tamai, M. Yamamoto, T. Taniguchi, K. Kishikawa, M. Kohri, Melanin precursor influence on structural colors from artificial melanin particles: PolyDOPA, polydopamine, and polynorepinephrine, Langmuir 34 (39) (2018) 11814–11821.

[18] S.H. Ku, J. Ryu, S.K. Hong, H. Lee, C.B. Park, General functionalization route for cell adhesion on non-wetting surfaces, Biomaterials 31 (9) (2010) 2535–2541.

[19] G. Cheng, S.J. Hao, X. Yu, S.Y. Zheng, Nanostructured microfluidic digestion system for rapid high-performance proteolysis, Lab Chip 15 (3) (2015) 650–654.

[20] S. Hong, J. Kim, Y.S. Na, J. Park, S. Kim, K. Singha, G. Il Im, D.K. Han, W.J. Kim, H. Lee, Poly(norepinephrine): ultrasmooth material-independent surface chemistry and nanodepot for nitric oxide, Angew. Chem. Int. Ed. 52 (2013) 9187–9191.

[21] S.K. Madhurakkat Perikamana, J. Lee, Y. Bin Lee, Y.M. Shin, E.J. Lee, A.G. Mikos, H. Shin, Materials from mussel-inspired chemistry for cell and tissue engineering applications, Biomacromolecules 16 (9) (2015) 2541–2555.

[22] J.H. Ryu, P.B. Messersmith, H. Lee, Polydopamine surface chemistry: a decade of discovery, ACS Appl. Mater. Interfaces 10 (9) (2018) 7523–7540.

[23] C.Y. Gao, Y.Y. Guo, J. He, M. Wu, Y. Liu, Z.L. Chen, W.S. Cai, Y.L. Yang, C. Wang, X.Z. Feng, -3,4-dihydroxyphenylalanine-collagen modified PDMS surface for controlled cell culture, J. Mater. Chem. 22 (2012) 10763–10770.

[24] X. Jiang, Y. Li, Y. Liu, C. Chen, M. Chen, Selective enhancement of human stem cell proliferation by mussel inspired surface coating, RSC Adv. 6 (2016) 60206–60214.

[25] J.L. Chen, J. Wang, P.K. Qi, X. Li, B.L. Ma, Z.Y. Chen, Q.L. Li, Y.C. Zhao, K.Q. Xiong, M.F. Maitz, N. Huang, Biocompatibility studies of poly(ethylene glycol)–modified titanium for cardiovascular devices, J. Bioact. Compat Polym. 27 (6) (2012) 565–584.

[26] Y. Yang, P.K. Qi, Y.H. Ding, M. Maitz, Z.L. Yang, Q.F. Tu, K.Q. Xiong, Y. Leng, N. Huang, A biocompatible and functional adhesive amine-rich coating based on dopamine polymerization, J. Mater. Chem. B. 3 (2015) 72–81.

[27] Z.L. Yang, Q.F. Tu, M. Maitz, S. Zhou, J. Wang, N. Huang, Direct thrombin inhibitor-bivalirudin functionalized plasma polymerized allylamine coating for improved biocompatibility of vascular devices, Biomaterials 33 (32) (2012) 7959–7971.

[28] P.K. Qi, W. Yan, Y. Yang, Y.L. Li, Y. Fan, J.Y. Chen, Z.L. Yang, Q.F. Tu, N. Huang, Immobilization of DNA aptamers via plasma polymerized allylamine film to construct an endothelial progenitor cell-capture surface, Colloids Surf., B 126 (2015) 70–79.

[29] J. Kuang, J.L. Guo, P.B. Messersmith, High ionic strength formation of DOPA-melanin coating for loading and release of cationic antimicrobial compounds, Adv. Mater. Interfaces. 1 (2014) 1400145.

[30] A. Havasian, E. Heydaripour, M.R. Nateghi, M.H. Mosslemin, F. Kalantari-Fotouh, Synthesis, characterization, and application of monodisperse poly L-Dopa microspheres, Turk. J. Chem. 42 (2018) 1370–1383.

[31] Z.Y. Xi, Y.Y. Xu, L.P. Zhu, Y. Wang, B.K. Zhu, A facile method of surface modification for hydrophobic polymer membranes based on the adhesive behavior of poly(DOPA) and poly(dopamine), J. Membr. Sci. 327 (1–2) (2009) 244–253.

[32] V. Ball, Physicochemical perspective on "polydopamine" and "poly(catecholamine)" films for their applications in biomaterial coatings (Review), Biointerphases 9 (3) (2014) 030801.

[33] T.A. Horbett, Fibrinogen adsorption to biomaterials, J. Biomed. Mater. Res. 106 (10) (2018) 2777–2788.

[34] M. Weber, H. Steinle, S. Golombek, L. Hann, C. Schlensak, H.P. Wendel, M. Avci-Adali, Blood-contacting biomaterials: in vitro evaluation of the hemocompatibility, Front. Bioeng. Biotechnol. 6 (2018) 99.

[35] M. Gorbet, C. Sperling, M. Maitz, C.A. Siedlecki, C. Werner, M.V. Sefton, The blood compatibility challenge. Part 3: material associated activation of blood cascades and cells, Acta Biomater. 94 (2019) 25–32.

[36] M. Zhang, T.A. Horbett, Tetraglyme coatings reduce fibrinogen and von Willebrand factor adsorption and platelet adhesion under both static and flow conditions, J. Biomed. Mater. Res. 89 (3) (2009) 791–803.

[37] C. Sperling, M. Maitz, S. Grasso, C. Werner, S. Kanse, A positively charged surface triggers coagulation activation through factor VII activating protease (FSAP), ACS Appl. Mater. Interfaces 9 (46) (2017) 40107–40116.

[38] P.E. Scopelliti, A. Borgonovo, M. Indrieri, L. Giorgetti, G. Bongiorno, R. Carbone, A. Podestà, P. Milani, The effect of surface nanometre-scale morphology on protein adsorption, PloS One 5 (7) (2010) e11862.

[39] R.A. Byrne, M. Joner, A. Kastrati, Stent thrombosis and restenosis: what have we learned and where are we going? the Andreas Grüntzig Lecture ESC 2014, Eur. Heart J. 36 (47) (2015) 3320–3331.

[40] X.Y. Li, P. Gao, J.Y. Tan, K.Q. Xiongm, M. Maitz, C.J. Pan, H.K. Wu, Y. Chen, Z.L. Yang, N. Huang, Assembly of metal-phenolic/catecholamine networks for synergistically anti-inflammatory, antimicrobial, and anticoagulant coatings, ACS Appl. Mater. Interfaces 10 (47) (2018) 40844–40853.

[41] S.H. Ku, C.B. Park, Human endothelial cell growth on mussel-inspired nanofiber scaffold for vascular tissue engineering, Biomaterials 31 (36) (2010) 9431–9437.

[42] S. Pacelli, P. Paolicelli, S. Petralito, S. Subham, D. Gilmore, G. Varani, G. Yang, D. Lin, M.A. Casadei, A. Paul, Investigating the role of polydopamine to modulate stem cell adhesion and proliferation on gellan gum-based hydrogels, ACS Appl. Bio Mater. 3 (2) (2020) 945–951.

[43] Z.L. Yang, Q.F. Tu, Y. Zhu, R.F. Luo, X. Li, Y. Xie, M. Maitz, J. Wang, N. Huang, Mussel-inspired coating of polydopamine directs endothelial and smooth muscle cell fate for re-endothelialization of vascular devices, Adv. Healthc. Mater. 1 (5) (2012) 548–559.

[44] M. Arka, B. Sankar, S. Santiswarup, P. Hirak, Inner-view of nanomaterial incited protein conformational changes: insights into designable interaction, Research (2018) 1–15.

[45] I.N. Serratos, R. Olayo, C. Millán-Pacheco, J. Morales-Corona, J.O. Vicente-Escobar, A.M. Soto-Estrada, J.G. Cordoba-Herrera, O. Uribe, T. Gomez-Quintero, M.A. Arroyo-Ornelas, R. Godinez-Fernandez, Modeling integrin and plasma-polymerized pyrrole interactions: chemical diversity relevance for cell regeneration, Sci. Rep. 9 (2019) 7009.

[46] J. Wang, K.F. Ren, H. Chang, F. Jia, B.C. Li, Y. Ji, J. Ji, Direct adhesion of endothelial cells to bioinspired poly(dopamine) coating through endogenous fibronectin and integrin α5β1, Macromol. Biosci. 13 (2013) 483–493.

[47] K.O. Mercurius, A.O. Morla, Inhibition of vascular smooth muscle cell growth by inhibition of fibronectin matrix assembly, Circ. Res. 82 (5) (1998) 548–556.

[48] M.L. Novak, T.J. Koh, Macrophage phenotypes during tissue repair, J. Leukoc. Biol. 93 (6) (2013) 875–881.

[49] M. Jaguin, N. Houlbert, O. Fardel, V. Lecureur, Polarization profiles of human M-CSF-generated macrophages and comparison of M1-markers in classically activated macrophages from GM-CSF and M-CSF origin, Cell, Immunol. 281 (1) (2013) 51–61.

[50] C.A. Ambarus, T. Noordenbos, M.J.H. de Hair, P.P. Tak, D.L.P. Baeten, Intimal lining layer macrophages but not synovial sublining macrophages display an IL-10 polarized-like phenotype in chronic synovitis, Arthritis Res. Ther. 14 (2) (2012) R74.

[51] I.U. Schraufstatter, M. Zhao, S.K. Khaldoyanidi, R.G. Discipio, The chemokine CCL18 causes maturation of cultured monocytes to macrophages in the M2 spectrum, Immunology 135 (4) (2012) 287–298.

[52] R. Sridharan, A.R. Cameron, D.J. Kelly, C.J. Kearney, F.J. O'Brien, Biomaterial based modulation of macrophage polarization: a review and suggested design principles, Mater. Today 18 (6) (2015) 313–325.

[53] S. Chen, J.A. Jones, Y. Xu, H.Y. Low, J.M. Anderson, K.W. Leong, Characterization of topographical effects on macrophage behavior in a foreign body response model, Biomaterials 31 (13) (2010) 3479–3491.

[54] K.M. Hotchkiss, G.B. Reddy, S.L. Hyzy, Z. Schwartz, B.D. Boyan, R. Olivares-Navarrete, Titanium surface characteristics, including topography and wettability, alter macrophage activation, Acta Biomater. 31 (2016) 425–434.

[55] D. Akilbekova, R. Philiph, A. Graham, K.M. Bratlie, Macrophage reprogramming: influence of latex beads with various functional groups on macrophage phenotype and phagocytic uptake in vitro, J. Biomed. Mater. Res. 103 (1) (2015) 262–268.

[56] J.M. Anderson, A. Rodriguez, D.T. Chang, Foreign body reaction to biomaterials, Semin. Immunol. 20 (2) (2008) 86–100.

[57] G. Wu, P. Li, H. Feng, X. Zhang, P.K. Chu, Engineering and functionalization of biomaterials via surface modification, J. Mater. Chem. B. 3 (2015) 2024–2042.

[58] W. Cheng, X. Zeng, H. Chen, Z. Li, W. Zeng, L. Mei, Y. Zhao, Versatile polydopamine platforms: synthesis and promising applications for surface modification and advanced nanomedicine, ACS Nano 13 (8) (2019) 8537–8565.

[59] Q.F. Tu, X.H. Shen, Y.W. Liu, Q. Zhang, X. Zhao, M. Maitz, T. Liu, H. Qiu, J. Wang, N. Huang, Z.L. Yang, A facile metal-phenolic-amine strategy for dual-functionalization of blood-contacting devices with antibacterial and anticoagulant properties, Mater. Chem. Front. 3 (2019) 265–275.

[60] H. Wang, C. Lin, X. Zhang, K. Lin, X. Wang, S.G. Shen, Mussel-inspired polydopamine coating: a general strategy to enhance osteogenic differentiation and osseointegration for diverse implants, ACS Appl. Mater. Interfaces 11 (7) (2019) 7615–7625.

[61] Y. Yang, P. Gao, J. Wang, Q.F. Tu, L. Bai, K.Q. Xiong, H. Qiu, X. Zhao, M. Maitz, H.Y. Wang, X.Y. Li, Q. Zhao, Y. Xiao, N. Huang, Z.L. Yang, Endothelium-mimicking multifunctional coating modified cardiovascular stents via a stepwise Metal-Catechol-(Amine) surface engineering strategy, Research (2020) 1–34.

[62] T. Liu, Z. Zheng, Y. Liu, J. Wang, M. Maitz, Y. Wang, S.H. Liu, N. Huang, Surface modification with dopamine and heparin/poly-L-Lysine nanoparticles provides a favorable release behavior for the healing of vascular stent lesions, ACS Appl. Mater. Interfaces 6 (11) (2014) 8729–8743.

[63] G. Li, B. Xie, C. Pan, P. Yang, H. Ding, N. Huang, Facile conjugation of heparin onto titanium surfaces via dopamine inspired coatings for improving blood compatibility, J. Wuhan Univ. Technol.-Materials Sci. Ed. 29 (4) (2014) 832–840.

[64] Q. Song, L. Li, K. Xiong, W. Tian, J. Lu, J. Wang, N. Huang, Q. Tu, Z. Yang, A facile dopamine-mediated metal-catecholamine coating for therapeutic nitric oxide gas interface-catalytic engineering of vascular devices, Biomater. Sci. 7 (2019) 3741–3750.